Macromolecules

ARTICLE

pubs.acs.org/Macromolecules

Crystal Structure Analysis of Ethylene−Tetrafluoroethylene Alternating Copolymer

Atushi Funaki,[†,‡] Suttinun Phongtamrug,[†,§] and Kohji Tashiro*[,†]

[†]Department of Future Industry-Oriented Basic Science and Materials, Graduate School of Engineering, Toyota Technological Institute, Tempaku, Nagoya 468-8511, Japan

[‡]Research and Development Division, Asahi Glass Co., Ltd., Yokohama, Kanagawa 221-8755, Japan

ABSTRACT: Crystal structure of ethylene (E)−tetrafluoroethylene (TFE) alternating copolymer of TFE 50 mol % content has been determined on the basis of 2-dimensional X-ray fiber diagram measured for the uniaxially oriented sample. Different from the unit cell parameters reported previously by several researchers, the newly proposed unit cell is of triclinic type with a = 8.46 Å, b = 5.67 Å, c (fiber axis) = 5.00 Å, α = 83.0°, β = 97.0°, and γ = 89.7° and the space group $P\bar{1}$. Two slightly deflected but essentially planar-zigzag chains are packed in the unit cell with the zigzag planes parallel to the $a + b$ direction. These two chains are connected by a point of symmetry and are packed upward and downward along the chain axis. In contrast to the relatively sharp X-ray equatorial line profile, the first and second layer line profiles are diffuse. At the same time a series of observed meridional 00l reflections are found to show relative intensity different from the regular chain packing structure. These hkl and 00l reflection profiles were found to be quantitatively reproduced by assuming an aggregation of regular domains with the c-axial translational disorder between them.

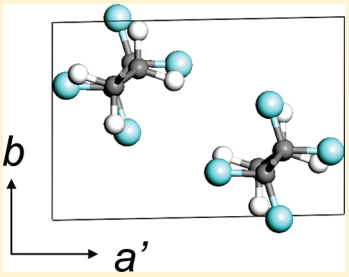

INTRODUCTION

Ethylene−tetrafluoroethylene (ETFE) alternating copolymer with molar content of E/TFE 50/50 mol % is used in the various application fields due to its excellent chemical stability, thermal stability, electric properties, and so on.[1] As reported by several researchers,[2−10] this copolymer exhibits the reversible phase transition at around 100 °C between the low-temperature and high-temperature phases, reflecting on the physical properties sensitively. Crystal structure and phase transition behavior are basically important for understanding the characteristic properties of the polymer. The whole scheme of the phase transition behavior of this ETFE copolymer is clarified relatively well. But, we have still one serious and not-yet-perfectly solved problem, which is needed to solve correctly for understanding the structural transition behavior in a concrete manner. The problem is to analyze the accurate crystal structure of this copolymer. The molecular chain conformation and the crystal structure of both the low- and high-temperature phases must be clarified with enough accuracy, in particular, the structure of the low-temperature phase as a starting point of discussion.

So far, several researchers reported the crystal structure of the low-temperature phase, but the correct answer is still ambiguous.[10−12] For example, Wilson and Starkweather proposed the monoclinic structure with space group $C2/m$-C_{2h}^3 and a = 9.6 Å, b = 9.2 Å, c (fiber axis) = 5.0 Å and γ = 96°, and also the structure of orthorhombic cell with space group $Cmca$-D_{2h}^{18}.[11] But they did not determine the structure through the quantitative comparison of X-ray diffraction intensities between the observed and calculated values. Tanigami et al. proposed the orthorhombic unit cell of a = 8.57 Å, b = 11.20 Å, and c (fiber axis) = 5.04 Å, in which four planar-zigzag chains were packed in a herringbone mode.[12] The setting angle of planar-zigzag chains was determined by comparing the observed and calculated intensity ratio of the two innermost equatorial X-ray reflections (120 and 200). But, their model does not give a good agreement between the observed and calculated intensities of many other reflections, as will be checked in a later section of the present paper. Besides, judging from the source, their sample is speculated to contain small amount of the third monomer content and it is not a purely two-component ETFE copolymer. Existence of the third component might affect the unit cell parameters as well as the X-ray diffraction pattern itself.[13] Phongtamrug et al. determined the unit cell parameters for a series of ETFE copolymers with various E/TFE contents.[10] Since the innermost reflection was found to be an overlap of two reflections of slightly different lattice spacings, their proposal of monoclinic unit cell might be reasonable. But they did not give any plausible crystal structure model in their paper.

In this way, the crystal structure of ETFE alternating copolymer has not yet been established enough satisfactorily. In the present paper, we have been challenged to reanalyze the crystal structure of ETFE 50/50 mol % copolymer on the basis of 2-dimensional X-ray fiber diagram taken for a uniaxially oriented sample. A new crystal structure model is proposed which can reproduce the observed X-ray diffraction profiles reasonably.

EXPERIMENTAL SECTION

Samples. ETFE alternating copolymer of 50/50 mol % was synthesized by a solution polymerization reaction of ethylene and tetrafluoroethylene monomers in hydrofluorocarbon used as a solvent.[14] The copolymer was melted (melting point 282 °C) and quenched into ice−water bath. This sample was stretched by about 3 times the original length at about

Received: December 7, 2010
Revised: January 31, 2011
Published: February 22, 2011

100 °C, followed by heat treatment at 250 °C for 3 h under tension. The thus-prepared uniaxially oriented sample of ca. 0.3 mm diameter was supplied to the X-ray diffraction measurement.

Measurements. The 2-dimensional X-ray diffraction pattern of the uniaxially oriented sample was measured using an X-ray beam of Mo Kα line from a Rigaku R-Axis Rapid II X-ray diffractometer equipped with an imaging plate detector of cylindrical shape (radius 127.4 mm). The X-ray diffraction measurements were performed at room temperature as well as at −100 °C by blowing cool nitrogen gas using a cryostat CryoMini Cold-head and a Rigaku temperature controller.

RESULTS AND DISCUSSION

Determination of Unit Cell Parameters. Figure 1 shows the 2-dimensional X-ray fiber pattern taken for uniaxially oriented ETFE sample at an ambient temperature as an example. The X-ray diffraction profiles scanned along the equatorial and layer lines are shown in Figure 2. The X-ray diffraction diagram was also measured at −100 °C, though it is not reproduced here. Almost no difference was found in the pattern between room temperature and −100 °C, except a slight shift of peak positions due to the thermal expansion. In particular, the diffuse first and second layer lines did not become sharper even at −100 °C. This suggests that the diffuse scatterings along the layer lines do not originate from the thermal motion of molecular chains but they come rather from the packing disorder of the chains as will be investigated in a later section.

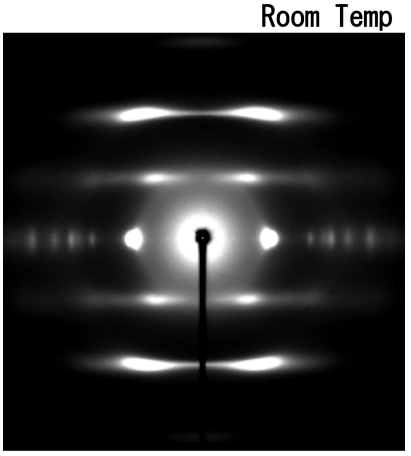

Figure 1. 2-Dimensional X-ray fiber pattern taken at an ambient temperature for the uniaxially oriented ETFE sample.

Since the layer line reflections are diffuse, it is difficult at the starting point to carry out the indexing of all the observed reflections, except the equatorial line. So the parameters of the unit cell projected along the chain axis (a', b', and γ') were determined by reading the positions of the observed equatorial reflections. Indexing of these reflections was performed by a trial-and-error method. The lattice parameters are as follows:

$$a' = 8.40\ \text{Å}, \quad b' = 5.63\ \text{Å}, \quad \gamma' = 88.8°$$

The indices and the lattice spacings are listed in Table 1 for all the observed equatorial reflections in comparison with the calculated lattice spacings.

The other unit cell parameters (α and β) may be determined through the fitting process of the whole X-ray diffraction profiles including the layer line reflections, and the analysis will be described in a later section. The fiber period along the chain axis was evaluated from the interlayer spacings, 5.00 Å. The molecular chain can be said approximately to take a planar-zigzag conformation, where the calculated fiber period is just 5.08 Å for the standard values of CC bond lengths (1.54 Å) and CCC bond angles (111.0°).

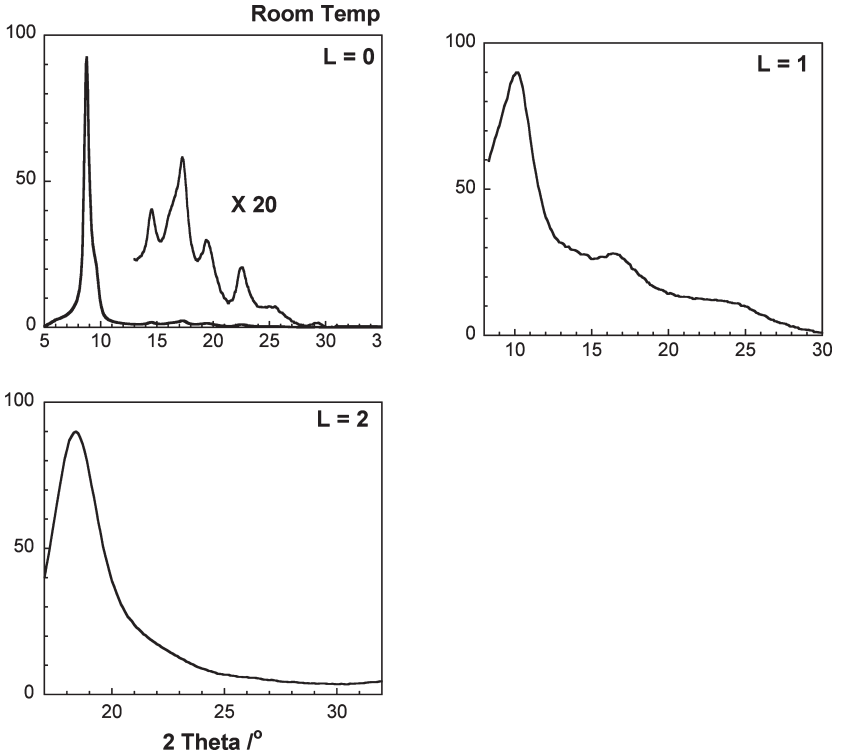

Figure 2. X-ray diffraction profiles scanned along the equatorial and layer lines in Figure 1.

dx.doi.org/10.1021/ma102785y |*Macromolecules* 2011, 44, 1540–1548

Table 1. Reflection Indices ($hk0$) and the Corresponding Lattice Spacings Evaluated for ETFE Copolymer

h	k	l	d_{obs}[a]/Å	d_{calc}[b]/Å
1	1	0	4.66	4.72
1	−1	0		4.63
2	0	0	4.33	4.20
0	2	0	2.81	2.81
3	1	0	2.49	2.53
3	−1	0		2.49
2	2	0	2.36	2.36
2	−2	0		2.32
4	0	0	2.10	2.10
1	3	0	1.82	1.84
1	−3	0		1.82
5	1	0	1.66	1.62
5	−1	0		1.60
0	4	0	1.41	1.41
6	0	0		1.40

[a] d_{obs}: lattice spacing obtained from the observed reflections. [b] d_{calc}: lattice spacing calculated from the unit cell parameters given in the text.

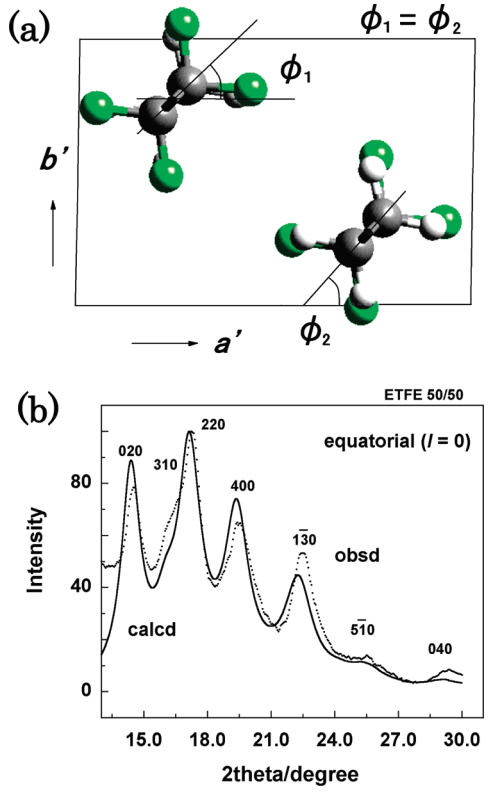

Figure 3. (a) Structural model of ETFE copolymer giving a good agreement of the X-ray equatorial line profile between the observed (—) and calculated (---) ones as shown in (b). The rigid planar-zigzag chains were assumed here.

Crystal Structure Models.

Structure Projected onto the Equatorial Plane. The observed density of the bulk sample d_{obs} was 1.70 g/cm^3. Since this polymer is an alternating copolymer, a repeating unit may be reasonably assumed to be $CH_2CH_2CF_2CF_2$ with the molecular weight M = 128 g/mol. Then the number of repeating units included in the unit cell Z was calculated to be 1.94. In other words, the two zigzag chains are included in a unit cell.

Table 2. Comparison between the Observed and Calculated Structure Factors along the Equatorial Line

h	k	l	F_{obs}	F_{calc}
1	1	0	49.85	46.00
1	-1	0		
2	0	0	27.83	30.76
0	2	0	9.70	10.19
3	1	0	7.48	8.88
3	-1	0		
2	2	0	16.24	19.07
2	-2	0		
4	0	0	12.83	12.75
1	3	0	11.25	16.25
1	-3	0		
5	1	0	10.29	8.57
5	-1	0		
0	4	0	4.95	3.60
6	0	0		

The X-ray equatorial diffraction profile is calculated for the packing model of these two zigzag chains in the unit cell, where the setting angles of the zigzag planes or the angle between the a'-axis and the zigzag plane must be determined reasonably so that the best agreement is obtained between the observed and calculated equatorial X-ray line profiles. The calculation was performed by using a commercial software Cerius^2 (version 4.6, Accelrys, Inc.). The crystallite size was assumed to be $L_a = L_b = L_c$ = 100 Å. The lattice strains were 2.0% for the a, b, and c directions. An isotropic temperature factor was 10.0 Å^2 in the ab plane and 5 Å^2 in the c direction for all the atoms.

After some trials, the most plausible model was found out which gave the relatively good reproduction of the observed equatorial line profile as shown in Figure 3. The two chains are packed with their zigzag planes parallel to the $(\bar{1}10)$ plane. In Figure 3b is compared the X-ray diffraction profile along the equatorial line between the observed and calculated ones.

The thus-obtained initial model was refined so that the agreement of X-ray diffraction profile along the equatorial line became the best in a quantitative manner. The structure factors F_{calc} were calculated as a function of setting angle ϕ of the zigzag plane measured from the a'-axis, where the molecular chains were assumed to be rigid (see Figure 3a). The calculation was made using a software of constrained least-squares method developed by ourselves. The degree of agreement of the X-ray diffraction profile was expressed using a reliability factor R:

$$R = (\sum||F_{obs}| - |F_{calc}||)/\sum|F_{obs}|$$

In this equation, $|F_{calc}|$ is the absolute value of the structure factor calculated from the observed reflection intensity: $|F_{obs}| = [I_{obs}/(KmpLA)]^{1/2}$, where I_{obs} is an observed intensity, K is a scale

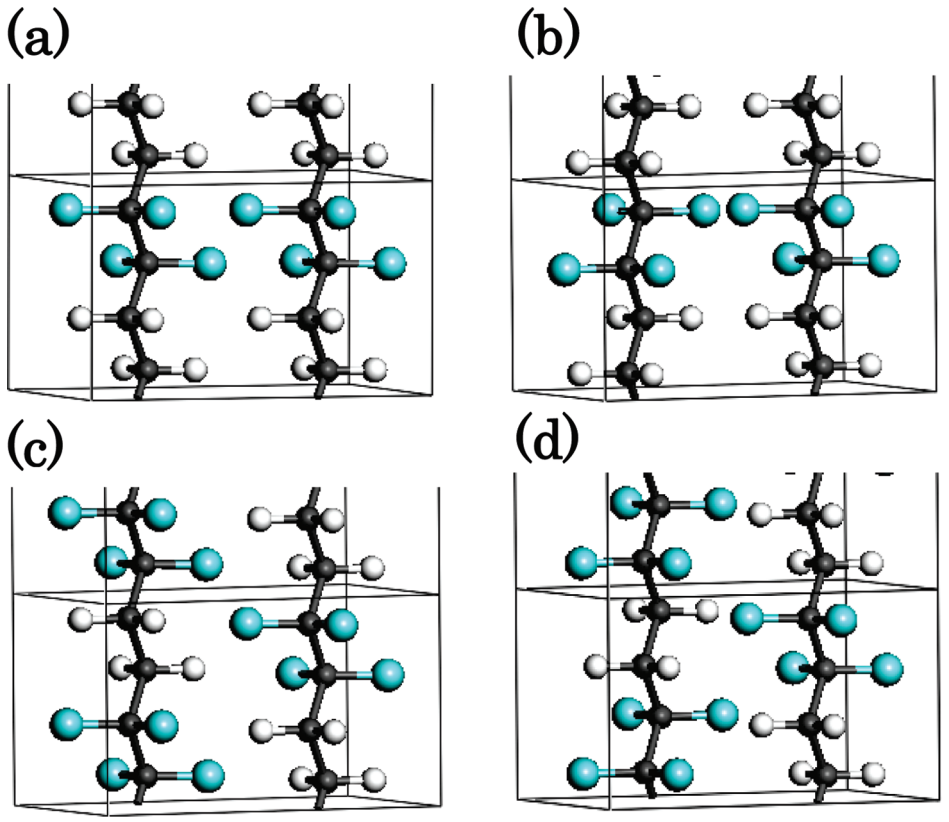

Figure 4. Four possible models of ETFE copolymer with the different relative height and orientation between the neighboring zigzag chains. (a) and (b): the relative height of CF_2CF_2 units is the same between the neighboring chains. (c) and (d): the relative height of CF_2CF_2 units between the neighboring chains is different by 0.5 along the *c*-axis.

factor, *m* is a multiplicity, *p* is a polarization factor, *L* is a Lorentz factor, and *A* is an absorption factor which was neglected here for the carbon and fluorine atoms. The setting angles ϕ_1 and ϕ_2 were found to take almost the common value of about 55°, giving the lowest *R* factor of about 18%.

Before we proceed with the structural refinement furthermore, we need to check the chain conformation itself. So far, the planar-zigzag conformation was assumed for finding out the most plausible packing structure since the observed fiber period or the *c*-axis length is close to the calculated value. But the chain conformation must not be necessarily restricted to the planar-zigzag form only. We might have a possibility of slightly deflected conformation as reported for poly(vinylidene fluoride) crystal form I.[15] The structural refinement was performed by modifying the chain conformation and chain packing mode in the triclinic unit cell. The variable parameters were the atomic coordinates and the isotropic temperature factors as well as the scale factor between the observed and calculated intensity. The reliability factor for the planar-zigzag chain conformation was *R* = 22.8% for the 15 equatorial reflections. The slightly deflected chain conformation gave *R* = 13.1%. The comparison in the structure factors of the equatorial reflections is made in Table 2. The concrete conformation is

$$-CH_2-CF_2-CF_2-CH_2-CH_2-$$
$$-185^\circ\ 190^\circ\ 175^\circ\ 170^\circ$$

3D-Packing Structure. So far, the structure model projected along the chain axis was searched since only the equatorial-line reflections can be used for the quantitative analysis. We need to develop this 2-dimensional structure to the 3-dimensional model by taking the layer line profiles into account. However, the layer lines are too diffuse to obtain the reasonable solution straightforwardly.

When the 2D-structure model is developed to the 3D model, we may have basically four possible models as illustrated in Figure 4. At first the α and β angles of the unit cell were assumed to be 90° for simplicity. Here we still assume the planar-zigzag chain models. In the first two models of Figure 4a,b, the CH_2CH_2 (and CF_2CF_2) groups of the neighboring chains are at the same height, but the orientation of these groups is parallel in (a) and antiparallel in (b). In the models (c) and (d), the CH_2CH_2 and CF_2CF_2 groups are arrayed face to face at the same height but in an opposite orientation. The X-ray reflection profile along the equatorial line is of course the same for all these four models. But, the layer line profiles are appreciably different from each other as shown in Figure 5. Among these models, the model (c) gives the calculated first and second layer lines consistent with the observed profile as a whole.

In this way, the model (c) has been known to give relatively good reproduction of the whole reflection profiles. However, as already mentioned above, the unit cell angles α and β were assumed to be 90°. The reflection positions are more or less deviated from the observed peak positions. Then all the unit cell parameters were modified but with keeping the structure projected along the chain (Figure 3a). The results are as follows:

$$a = 8.46\ \text{Å},\quad b = 5.67\ \text{Å},\quad c = 5.00\ \text{Å},$$
$$\alpha = 83.0^\circ,\quad \beta = 97.0^\circ,\quad \gamma = 89.7^\circ$$

Referring to the most plausible packing model given in Figure 4c, the possible space group might be $P\bar{1}$-C_i.[16] The two neighboring chains are related to each other by a point of symmetry.

dx.doi.org/10.1021/ma102785y |*Macromolecules* 2011, 44, 1540–1548

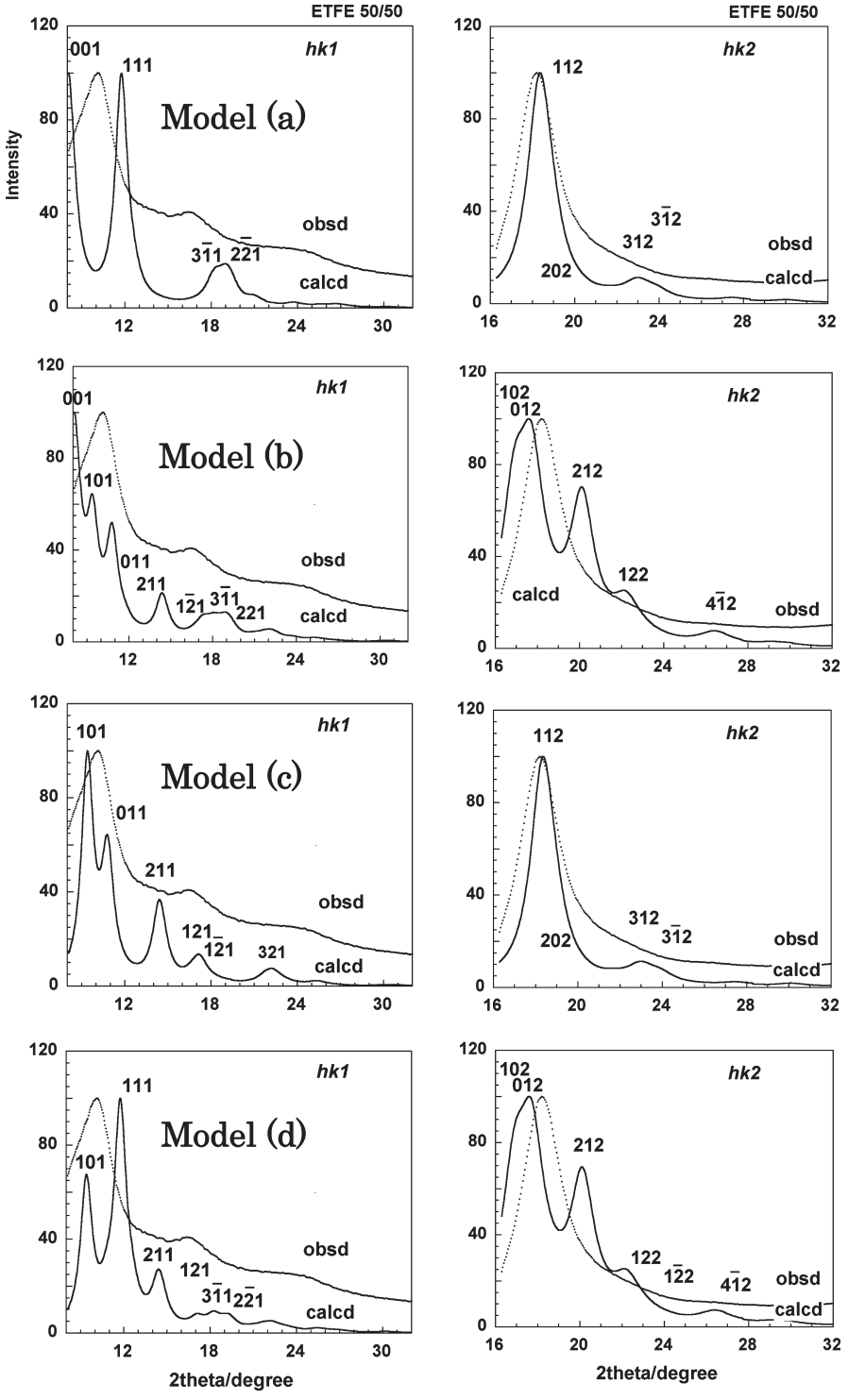

Figure 5. X-ray diffraction profiles along the first and second layer lines calculated for the four models given in Figure 4. The observed profiles are shown by broken lines. The model (c) gives the best agreement with the observed data.

Here we need to consider the 00*l* meridional reflections also for confirming the structural model. As reproduced in Figure 6, a Weissenberg diffraction pattern was measured by Norman's method where the drawn sample was rotated around the axis perpendicular to the draw axis so that the meridional 00*l* reflections were detected.[17] Figure 7a shows the observed profile of the 00*l* reflections, where the 004 reflection is detected strongly, whereas the 001−003 reflections are relatively weaker. In the above paragraphs we mentioned that the model (c) gives relatively good reproduction of the *hk*0, *hk*1, *and hk*2 reflection profiles as a whole. But, this model has to satisfy an intensity relation between a series of 00*l* reflections at the same time, in particular the strongest 004 reflection. The 00*l* reflection intensity is affected sensitively by the relative height of the neighboring chains in the unit cell. By changing the relative height (Δz) of the neighboring chains in the model (c), the 00*l* reflections were calculated using Cerius[2] software. Many models gave the strongest 001 reflection, and

dx.doi.org/10.1021/ma102785y |*Macromolecules* 2011, 44, 1540–1548

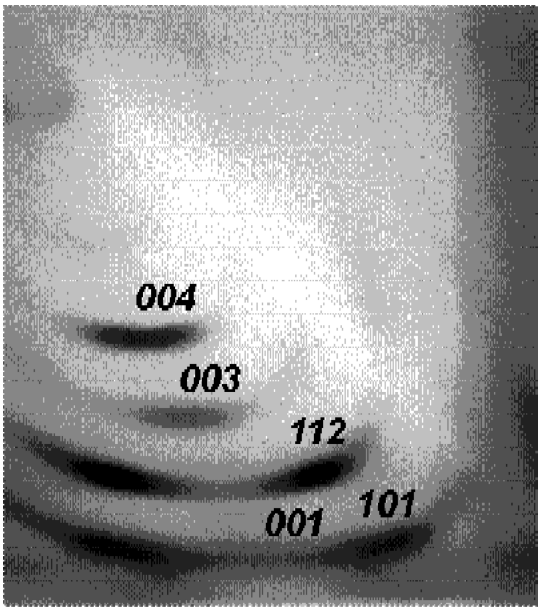

Figure 6. Weissenberg X-ray diffraction pattern taken for a uniaxially oriented ETFE copolymer using a Norman method, where the 00*l* reflections were measured by rotating the sample around the axis perpendicular to the drawn direction.

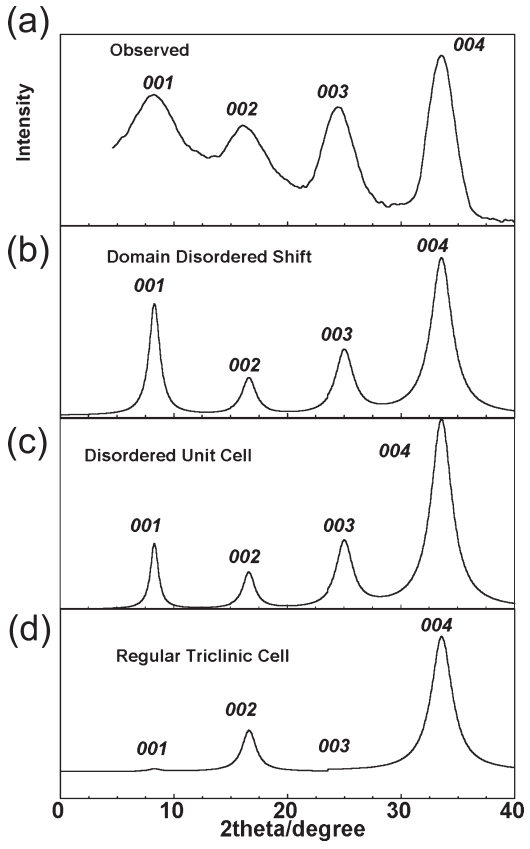

Figure 7. X-ray diffraction profile along the 00*l* direction. (a) The observed data, (b) the profile calculated for the *c*-axial translational disorder model of domain units (refer to Figure 9a), (c) the profile calculated for random *c*-axial translational model of chains in the crystallite, and (d) the profile calculated for the regular triclinic structure given in Figure 8.

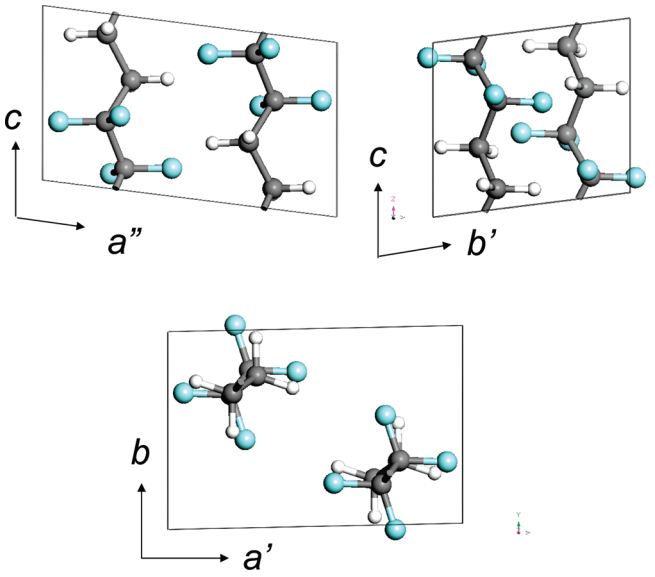

Figure 8. Finally determined unit cell structure of ETFE alternating copolymer.

only one unique model was found to give relatively good reproduction of strong 004 reflection intensity, which is given in Figure 8 where the relative height of the neighboring chains is $\Delta z \sim 0.0$. The thus-obtained model can satisfy also the observed *hk*0, *hk*1, and *hk*2 reflection profiles in addition to the strongest 004 reflections. Unfortunately, however, this model cannot give still enough satisfactory reproduction of all the 00*l* reflection intensities as seen in Figure 7d. That is to say, the 002 reflection is relatively strong and the 001 and 003 reflections are weaker, inconsistent with the observed tendency. This tendency cannot be reproduced at all by the structural model given in Figure 8 even when the chain packing mode was furthermore modified in many ways. In other words, the model given in Figure 8 seems to be the most plausible structure of ETFE 50/50 copolymer *as long as the regular packing structure is considered*. Introduction of structural disorder will be discussed in a later section. The atomic fractional coordinates of the thus established basic structural model are listed in Table 3.

Disorder in Relative Height of Chains. As pointed out above, the most plausible regular crystal structure shown in Figure 8 does not give a good reproduction of the relative intensity for a series of 00*l* reflections as seen in Figure 7d: the 002 reflection shows the stronger intensity compared with those of the 001 and 003 reflections. At the same time we must notice relatively strong diffuse scatterings along the layer lines (Figure 1). This comes from the disorder of chains with respect to the relative height of the chains along the chain axis. For the introduction of such a translational disorder along the chain axis, we might have at least two types of structural model: (i) a random shift of chains in the unit cell and (ii) random shift of crystalline domains along the chain axis with keeping the regular chain packing in the domain itself. The first model (i) is inconsistent with the above-mentioned regular triclinic structure shown in Figure 8. But, as a trial, we created one large cell consisting of 4 × 4 unit cells and arbitrary chains were shifted their relative height randomly along the chain axis. The resultant X-ray 00*l* reflection profile is shown in Figure 7c, giving a relatively good reproduction of the observed data. But, as mentioned above, this random shift violates the regular triclinic structure in Figure 8. The relatively good reproduction of 00*l* reflection profile using the model

Table 3. Atomic Fractional Coordinates of ETFE Structure Model (Figure 8)

atom[a]	*x*	*y*	*z*
C1	0.278	0.797	0.124
C2	0.214	0.675	0.380
C3	0.300	0.767	0.634
C4	0.217	0.679	0.884
F5	0.437	0.783	0.159
F6	0.221	1.025	0.083
F7	0.262	0.447	0.421
F8	0.054	0.688	0.345
H9	0.422	0.702	0.667
H10	0.298	0.958	0.606
H11	0.219	0.487	0.914
H12	0.095	0.744	0.852

[a] Numbering of atoms is shown below.

$$\begin{array}{cccccccc} & F_5 & & F_7 & & H_9 & & H_{11} \\ & | & & | & & | & & | \\ - & C_1 & - & C_2 & - & C_3 & - & C_4 & - \\ & | & & | & & | & & | \\ & F_6 & & F_8 & & H_{10} & & H_{12} \end{array}$$

[b] The unit cell parameters are a = 8.46 Å, b = 5.67 Å, c = 5.00 Å, α = 83.0°, β = 97.0°, and γ = 89.7° at room temperature. [c] The temperature factors are 10.0 Å^2 for the a and b directions and 5.0 Å^2 for the c direction.

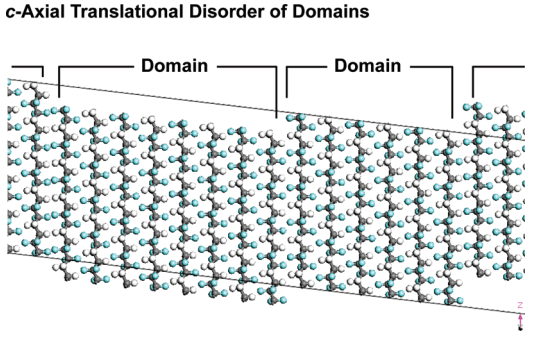

Figure 9. A model composed of finite domains with disordered translational shift along the chain axis which gives the relatively good reproduction of *hk*0, *hk*1, *hk*2, and 00*l* reflection profiles (refer to Figure 7b and Figure 10). The domain size was assumed properly. The domains were assumed to be arrayed along the *a*-axis. Of course, the domains can exist along the *b* direction or in any direction.

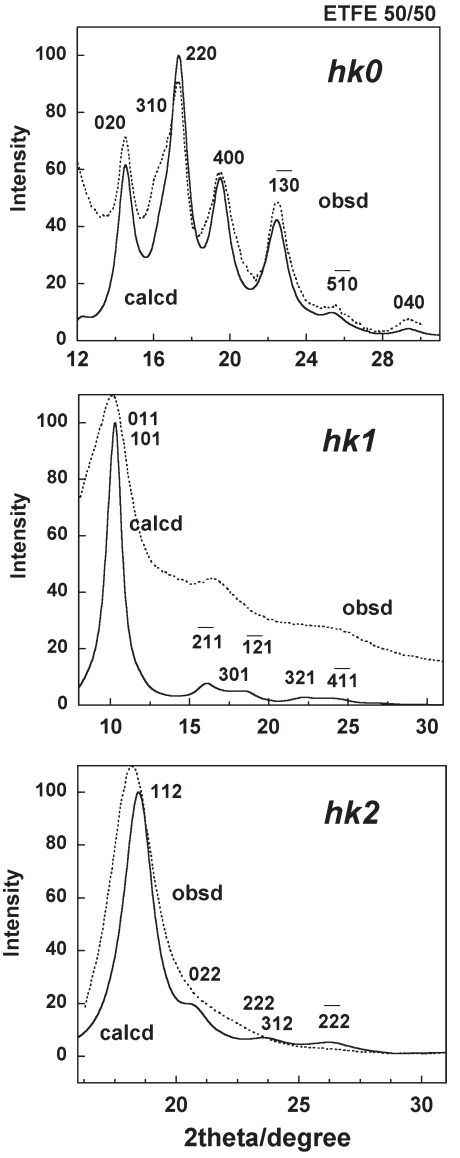

Figure 10. Comparison of X-ray diffraction profiles of ETFE copolymer along the equatorial, the first and second layer lines between the observed (broken lines) and the calculated ones (solid lines). The calculation was made for the structurally disordered model shown in Figure 9.

(i) suggests that an introduction of randomness is needed in order to attain a good reproduction of observed X-ray data. But, we have to keep in mind that that the regular chain packing in the unit cell must be also reserved at the same time. The second model (ii) or the translational shift of domains satisfies these requirements reasonably. This model can keep the regular unit cell structure in each domain, and it introduces also the irregularity into the crystallite as a whole by shifting the domain height randomly. Of course, these domains must be X-ray coherent. As a trial, the model given in Figure 9 was created and the X-ray diffraction profiles were calculated. In this model, one domain includes about eight chains along the *a*-axis. In the present trial the *b*-axis was assumed not to be shifted. This was because the 00*l* reflection intensities were governed by only the relative height of the chains. The 00*l* reflection profile shown in Figure 7b was obtained by this model: the 001 and 003 reflection intensities become stronger and the 002 reflection becomes weaker, reproducing the observed data relatively well. Of course, the observed data itself is not very much faithful as for the relative intensity among a series of 00*l* reflections because the streak scatterings overlap the meridional reflections more or less as understood from Figure 6. In such a sense, the relative height between the 001 and 003 cannot be said to be comparable or different from each other. What we can tell here is that the relative intensity is in the order of 004 ≫ 001 ≥ 003 > 002. This tendency was reproduced well by an introduction of translational height disorder of the neighboring domains. This type of disorder does not modify the X-ray diffraction profiles along the layer lines very much as reproduced in Figure 10, where the calculated *hk*0, *hk*1, and *hk*2 reflection profiles are compared with the observed data. Figure 11 gives the corresponding 2-dimensional X-ray

dx.doi.org/10.1021/ma102785y |*Macromolecules* 2011, 44, 1540–1548

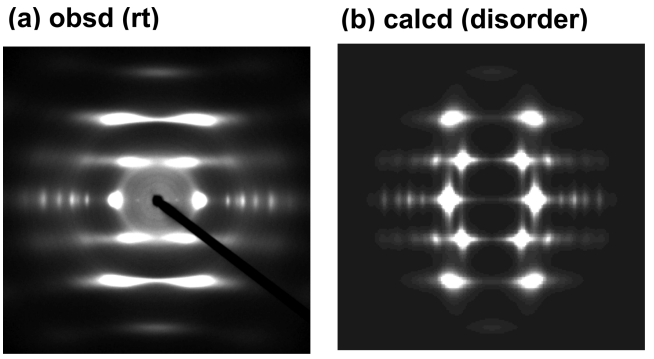

Figure 11. Observed and calculated X-ray fiber diagrams of uniaxially oriented ETFE copolymer. The calculation was made for the model shown in Figure 9a.

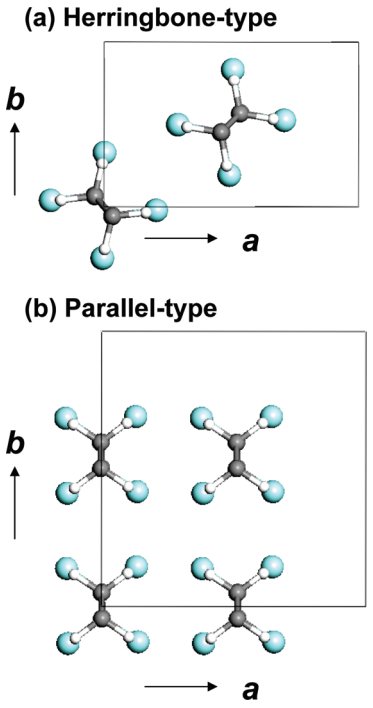

Figure 12. Crystal structures proposed by the previous researchers: (a) a herringbone-type model proposed by Tanigami et al.[12] and (b) a parallel-type model proposed by Wilson and Starkweather.[11]

diffraction pattern calculated for the model of Figure 9, consistent with the observed pattern.

In the model of Figure 9, the *c*-axial translational shift was made only along the *a* axial direction, but the situation is the same also for the *b*-axial direction since the 00*l* reflections are governed by only the relative height of the chains along the *c* axis. The translational shift of the domains may occur in both the *a* and *b* directions or even in an arbitrary direction. Of course, however, the energetic preferability of domain boundary is needed to be considered for the realization of the actual aggregation structure of multiple domains. The details should be a future work.

At the final stage of this discussion, we want to add another possible origin of the broad lines, which may be the partial irregularity of monomer sequences along the polymer chain. For example, in addition to the regularly alternating sequences of ...-E-TFE-E-TFE-..., there might be irregular sequences such as ...−E−TFE−E−E−TFE−... or ...−TFE−E−TFE−TFE−E−.... The layer line profiles were calculated by introducing these chemical irregularities into the models. They did not give any good reproduction of the layer line profiles. That is to say, the chemical irregularity does not affect very much as long as the ETFE content is close to 50 mol %. The effect of chemical irregularity can be detected more clearly in the X-ray diffractions of the copolymers with higher or lower E/TFE ratio.[10]

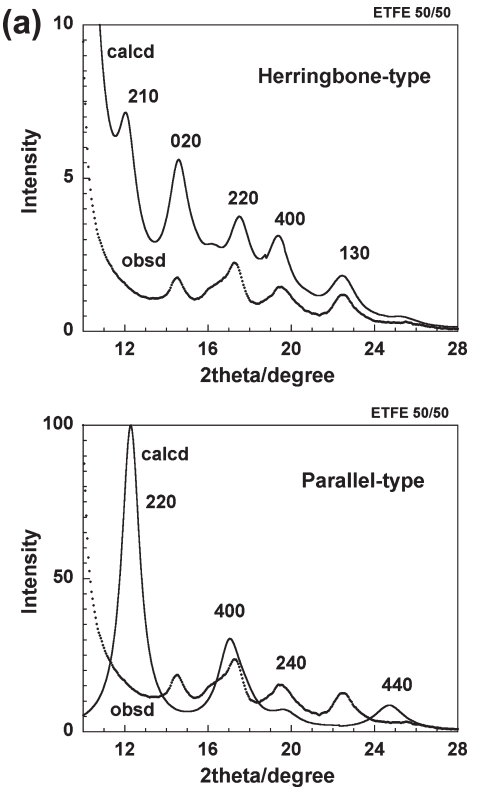

Figure 13. Comparison of the observed X-ray diffraction profile along the equatorial line with the profiles calculated for the models of (a) herringbone type (Figure 12a) and (b) parallel type (Figure 12b). The profiles were calculated repeatedly to obtain as good agreement with the observed data as possible.

Comparison of Various Crystal Structure Models. The crystal structure analyzed here is compared with those proposed by the previous researchers as shown in Figure 12. In the structure (b) proposed by Wilson and Starkweather[11] the perfectly planar-zigzag chains are packed in parallel along the *b*-axis in the unit cell with different values from ours. The unit cell parameters reported by Tanigami et al.[12] are close to ours, but they proposed a rectangular unit cell shape of orthorhombic type as shown in Figure 12a. The planar-zigzag chains are packed in the so-called herringbone mode, where the zigzag chains are packed with the zigzag planes almost perpendicular to each other ($\phi_2 = \phi_1 + 90°$ in Figure 3). As mentioned above, the X-ray diffraction profiles of this model were not checked by themselves. Both of these two models did not give a good reproduction of the observed X-ray diffraction data even after many trials were made by changing the setting angles of the chains as well as the modification of the unit cell parameters from their proposed ones so that the good agreement could be obtained as much as possible. But both of these models were impossible to reproduce the observed X-ray profiles reasonably as shown in Figure 13.

dx.doi.org/10.1021/ma102785y |*Macromolecules* 2011, 44, 1540–1548

CONCLUSION

In the present paper we reported the crystal structure of ETFE alternating copolymer on the basis of detailed analysis of the 2D X-ray diffraction pattern. Different from the crystal structure models proposed in the previous papers,[11,12] our newly proposed triclinic model consists of the two essentially planar-zigzag but slightly deflected chains, which are packed along the $1\bar{1}0$ plane of the triclinic unit cell ($P\bar{1}$-C_i). This model reproduces the observed X-ray diffraction profiles well. The 00*l* reflection profile and the broad layer line profiles can be reproduced reasonably by introducing the statistically random *c*-axial translational disorder of the neighboring domains with finite side.

The ETFE copolymer exhibits the transitions between the low- and high-temperature phases. In the present paper the crystal structure of the low-temperature phase has been analyzed. The crystal structure of the high-temperature phase may be derived by introducing the conformational and packing-mode disorders into the crystal structure of the low-temperature phase, leading to the pseudohexagonal phase.[12] The concrete analysis is now being processed.

AUTHOR INFORMATION

Corresponding Author

*E-mail: ktashiro@toyota-tiac.jp.

Present Addresses

[§]Faculty of Applied Science, King Mongkut's University of Technology North Bangkok, Bangsue, Bangkok 10800, Thailand.

ACKNOWLEDGMENT

This study was financially supported by a MEXT "the International Project on the Basic Research Promotion for the Development of Highly-Controlled Multi-Purpose Polymer Materials" in "the Strategic Project to Support the Formation of Research Bases at Private Universities" (2010−2014).

REFERENCES

(1) Drobnt, J. *Rapra Rev. Rep.* **2006**, *16*, 184.
(2) Pieper, T.; Heise, B.; Wilke, W. *Polymer* **1989**, *30*, 1768–75.
(3) Tanigami, T.; Yamamura, K.; Matsuzawa, S.; Ishikawa, M.; Mizoguchi, K.; Miyasaka, K. *Polymer* **1986**, *27*, 1521–8.
(4) Iuliano, M.; De Rose, C.; Guerra, G.; Petraccone, V.; Corradini, P. *Macromol. Chem.* **1989**, *190*, 827–35.
(5) Petraccone, V.; De Rosa, C.; Guerra, G.; luliano, M.; Corradini, P. *Polymer* **1992**, *33*, 22–6.
(6) Gal'perin, Y. L.; Tsvankin, D. Y. *Vysokomol. Soyed.* **1976**, *A18*, 2691–9.
(7) Phongtamrug, S.; Tashiro, K.; Arai, K.; Funaki, A.; Aida, S. *Polymer* **2008**, *49*, 561–9.
(8) D'Aniello, C.; De Rosa, C.; Guerra, G.; Petraccone, V.; Corradini, P.; Ajroldi, G. *Polymer* **1995**, *36*, 967–73.
(9) De Rosa, C.; Guerra, G.; D'Aniello, C.; Petraccone, V.; Corradini, P.; Ajroldi, G. *J. Appl. Polym. Sci.* **1995**, *56*, 271–8.
(10) Phongtamrug, S.; Tashiro, K.; Arai, K.; Funaki, A.; Aida, S. *Polymer* **2008**, *49*, 5072–83.
(11) Wilson, F. C.; Starkweather, H. W., Jr. *J. Polym. Sci., Part A-2* **1973**, *11*, 919–27.
(12) Tanigami, T.; Yamamura, K.; Matsuzawa, S.; Ishikawa, M.; Mizoguchi, K.; Miyasaka, K. *Polymer* **1986**, *27*, 999–1006.
(13) Funaki, A.; Arai, K.; Aida, S.; Phongtamrug, S.; Tashiro, K. *Polymer* **2008**, *49*, 5497–5503.
(14) Funaki, A.; Takakura, T.; Kato, K.; Hamazaki, K. JP3305400.
(15) Hasegawa, H.; Takahashi, T.; Chatani, Y.; Tadokoro, H. *Polym. J.* **1972**, *3*, 591–9.
(16) *International Table for Crystallography*; D. Reidel Publishing Co.: Dordrecht, 1983; Vol. A, p 133.
(17) Tadokoro, H. *Structure of Crystalline Polymers*; Robert E. Krieger Pub. Co.: Malabar, FL, 1990; p 136.